Analytical Expressions for Antenna on-Chip Efficiency at mm-Wave and Sub-THz Frequencies

Louis Delait, Christophe Craeye, Jean-Pierre Raskin, Dimitri Lederer

ICTEAM, Université catholique de Louvain, Belgium

{louis.delait, christophe.craeye, jean-pierre.raskin, dimitri.lederer}@uclouvain.be

***Abstract* — This paper aims to propose a systematic analysis tool for computing the efficiency of Antenna on-Chip (AoC) while prior knowledge on the material stack and current distribution is available. The aim of this work is twofold. First, the developed analytical expressions may enable AoC designers to evaluate antenna efficiency and effectively compare design options during the predesign phase without relying extensively on numerous full-wave simulations. Second, the proposed tool allows one to quantify the impact of each loss source in the AoC design: surface waves and material ohmic/dielectric losses. Expressions for AoC efficiency are derived in this paper for two widely used antenna types —patch and dipole antennas with current distributions following a truncated sine pattern— but the methodology is generalizable to any current distribution and lossy material stack. The model is validated with full-wave simulation for both a shielded and unshielded silicon chip stack with typical dimensions (i.e. with and without a metal plane shielding the antenna from the substrate) up to 350 GHz.**

***Keywords* — Antenna on-Chip, Antenna Efficiency, Substrate Resistivity, Dipole Antenna, Patch Antenna, Millimeter-Wave, Sub-THz, System on-Chip.**

I. Introduction

The quest for high data rates and high-resolution radar has recently drawn significant attention to millimeter-wave (mm-Wave) and sub-THz frequencies. Antennas on-Chip (AoC) enable direct integration with front-end circuitry, reducing connection loss and parasitic effects while facilitating co-design and are therefore a promising candidate for this frequency range [1], [2]. However, one of the primary challenges limiting their widespread adoption is their low efficiency, which is due to the unique physical and material constraints of on-chip environment [3]–[5].

Despite the critical role of efficiency in determining AoC performance, there has been no dedicated study to analyze the efficiency of canonical on-chip antennas, nor have analytical expressions been developed to quantify it. This paper introduces a systematic analysis tool for evaluating the efficiency of AoC, leveraging prior knowledge of the material stack and current distribution, which is typically available in most AoC design scenarios.

Several publications have proposed analytical expressions for the efficiency of canonical resonant planar antennas [6]–[8]. These studies generally assume a lossless antenna on a single lossless grounded dielectric layer, considering only coupling into surface wave (SW) as losses. This work extends that methodology to account for antennas lying on lossy multi-layer stacks and incorporates the conductive losses of the antenna itself. This extension is particularly relevant as typical chip stacks consist of multiple layers of lossy materials, and as demonstrated in this paper, material losses can significantly impact the efficiency of AoC designs.

The aim of this work is twofold. First, the developed analytical expressions may enable AoC designers to evaluate antenna efficiency and effectively compare design options during the predesign phase without relying extensively on numerous full-wave simulations. Second, the proposed tool quantifies the impact of each loss mechanism in AoC designs, including SW and material losses arising from substrate conductivity, dielectric loss tangent, or the finite conductivity of metals in the back-reflector and the antenna itself. This approach may then enable a rapid identification of the impact of each loss source and highlights potential design levers for improving efficiency.

Expressions are derived in this paper for two widely used antenna types —patch and dipole antennas with rectangular current distributions following a truncated sine pattern— but the methodology is generalizable to any current distribution and lossy material stack. The expressions of the efficiency developed in this paper are not closed form but only imply numerical integration that can be quickly evaluated using any programming tool in a few seconds on a laptop.

This paper is organized as follows: Section II develops the mathematical framework for the proposed efficiency analytical expression. Then, the methodology is demonstrated for a conventional silicon chip stack. In Section III, it is applied to unshielded AoC (i.e. metal plane below the Si substrate) and the impact of substrate resistivity on antenna efficiency is investigated. In Section IV, the case of shielded AoC is analyzed (i.e. a metal plane is separating the Back-end-of-Line (BEOL) from the substrate).

II. Mathematical Formalisation

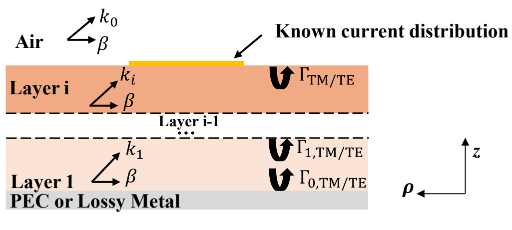

Fig. 1. Multi-layer stack scheme.

Considering a multi-layer stack, as shown in Fig. 1, with a lossless sheet antenna at the uppermost layer/air interface, the time average active power that leaves out this antenna can be expressed as

$$P_{out} = \mathbb{R}\left\{\frac{-1}{8\pi^2}\iint \widetilde{\boldsymbol{E}}\cdot\widetilde{\boldsymbol{J}}^*\, dk_x\, dk_y\right\} \tag{1}$$

with J the current density on the sheet and E the electric field due to this current. Both quantities are in the Fourier Domain. An equivalent expression is given in [8] in the spatial domain. The integration is performed in the Fourier domain such that the dyadic Green's function **G** can be expressed in closed form for a multi-layer stack, as shown in Fig. 1, for which all the layer permittivity values and thicknesses are supposed to be known. Equation (1) then becomes

$$P_{out} = \mathbb{R}\left\{\frac{-1}{8\pi^2}\iint \widetilde{\boldsymbol{G}}\widetilde{\boldsymbol{J}}\cdot\widetilde{\boldsymbol{J}}^*\, dk_x\, dk_y\right\}. \tag{2}$$

This paper focuses on rectangular current distributions following a truncated sine pattern (i.e. dipole or patch at first resonance). Supposing a current sheet along $\widehat{\boldsymbol{x}}$, of length L, width W and amplitude J_0 in Ampere, the current density on the sheet can be expressed as

$$J_x(x,y) = \begin{cases} J_0 \sin\left(\frac{\pi x}{L}\right)/W & 0<x<L\,, -\frac{W}{2}<y<\frac{W}{2} \\ 0 & \text{otherwise}\end{cases} \tag{3}$$

and its Fourier transform (as defined in [8]) as

$$\tilde{J}_x(k_x,k_y) = J_0\,\frac{2\frac{\pi}{L}\cos\left(\frac{L\,k_x}{2}\right)}{k_x^2-\left(\frac{\pi}{L}\right)^2}\,\frac{\sin(w\,k_y/2)}{w\,k_y/2}. \tag{4}$$

As the current is along x, the only needed Green's function component is $\tilde{G}^{xx}$, which links $\tilde{E}_{\boldsymbol{x}}$ to $\tilde{J}_{\boldsymbol{x}}$. It can be expressed in the Fourier domain, as explained in [9], as

$$\tilde{G}^{xx} = -\frac{\sin^2(\phi)}{D_{TE}(\beta)} - \frac{\cos^2(\phi)}{D_{TM}(\beta)} \tag{5}$$

with $D_{TE}(\beta)$ and $D_{TM}(\beta)$ defined in [10]. For the stack shown in Fig. 1, they can be expressed as

$$D_{TE}(\beta) = \frac{1}{k_0\eta_0}\left(k_{z,0} + k_{z,i}\,\frac{1-\Gamma_{\mathrm{TE}}}{1+\Gamma_{\mathrm{TE}}}\right) \tag{6.a}$$

$$D_{TM}(\beta) = \frac{k_0}{\eta_0}\left(\frac{1}{k_{z,0}} + \frac{\varepsilon_{r,i}}{k_{z,i}}\,\frac{1+\Gamma_{\mathrm{TM}}}{1-\Gamma_{\mathrm{TM}}}\right) \tag{6.b}$$

where β is the transverse wave vector and ϕ the azimuthal angle in the Fourier domain such that $k_x = \beta\cos(\phi)$, $k_y = \beta\sin(\phi)$. Respectively, k_0 and η_0 are the free space wave vector and impedance of the air. For a layer n, the z-oriented component of the wave vector is given by $k_{z,n} = \pm\sqrt{\varepsilon_{r,n}k_0^2 - \beta^2}$, where the sign + is chosen except for $k_{z,0}$, in the air, as it will be discussed. Γ_{TE} and Γ_{TM} are the reflection coefficients at the uppermost interface, computed recursively from $\Gamma_{0,\mathrm{TE}}$ and $\Gamma_{0,\mathrm{TM}}$ as defined in Fig. 1 [10].

The contribution due to radiation into free space comes mathematically from the range of integration $k_x^2 + k_y^2 < k_0^2$ [7], [8], that is the visible region. The physical meaning is that for each (k_x, k_y) pair in this region, $k_{z,0} = \sqrt{k_0^2 - k_x^2 - k_y^2}$ is real, meaning that energy is leaving the structure towards the air region. The radiated power can be computed by integrating the far field expression of the pointing vector of the radiated wave on the upper hemisphere as:

$$P_{rad} = \int_0^{2\pi}\int_0^{\frac{\pi}{2}} \frac{|E_\theta|^2+|E_\phi|^2}{2\eta_0} R^2 \sin(\theta)\, d\theta\, d\phi \tag{7}$$

with R the distance from the source and θ the elevation angle. The radiated $\bar{E} = E_\theta\hat{e}_\theta + E_\phi\hat{e}_\phi$ in the upper region given by [8]:

$$\bar{E} = \frac{jk_0\, e^{-jk_0R}}{2\pi R}\tilde{J}_x(\theta,\phi)\left(\frac{\cos(\theta)\sin(\phi)}{D_{TE}(\theta,\phi)}\hat{\boldsymbol{e}}_{\boldsymbol{\phi}} + \frac{\cos(\phi)}{D_{TM}(\theta,\phi)}\hat{\boldsymbol{e}}_{\boldsymbol{\theta}}\right) \tag{8}$$

In the lossless case, the surface wave power can be found from the residue at the surface wave poles which occurs when the functions $D_{TM}(\beta)$ and $D_{TE}(\beta)$ of (5) vanish [9]. If above cut-off frequency of the corresponding modes, $D_{TM}(\beta)$ gives rise to the TM SW modes of which TM_0 is the fundamental (no cut-off) and $D_{TE}(\beta)$ gives rise to the TE SW modes. Extracting the residue requires then to compute the value of the pole for a multi-layer stack. From the residue extraction, in the general case of a multi-layer stack, the power coupled from a real current distribution oriented along $\widehat{\boldsymbol{x}}$ to the TM_0 mode can be shown to be equal, using l'Hospital's rule, to

$$P_{TM0} = \mathbb{R}\left\{\frac{-j}{8\pi}\int_0^{2\pi}\frac{N(\beta_{TM0})}{D'(\beta_{TM0})}\beta_{TM0}\cos^2(\phi)\,\left|\tilde{J}_x\right|^2 d\phi\right\} \tag{9}$$

with $1/D_{TM}(\beta) = N(\beta)/D(\beta)$, and β_{TM0} the propagation constant of the TM_0 SW mode. This term accounts for all the power coupled to SW while the considered frequency is below the cut-off of the first higher order mode, TE_1. A similar expression can be found in [7] for the case of an infinitesimal electric dipole current on a lossless single-layer grounded slab.

In a more general way, it is possible to catch the surface wave power of all the modes in the lossless case by numerically estimating the integral in (2) in the invisible region, which corresponds to the integration range $k_x^2 + k_y^2 > k_0^2$, including the SW singularities. In the invisible region the negative square root $k_{z,0} = -\sqrt{k_0^2 - k_x^2 - k_y^2}$ should be selected to avoid field divergence as z tends towards $+\infty$.

It should be noted that the residue is the only contributor to the SW power in (1) in the lossless case, as it can be shown that the Cauchy's principal value, as detailed in (87) of [9], only corresponds to the radiated power.

The losses in the multi-layer stack can be accounted for by considering complex values of permittivity in $\tilde{G}^{xx}$ such that the complex relative permittivity of the layer i can be expressed as $\varepsilon'_{r,i} = \varepsilon_{r,i} - j\frac{\sigma_i}{\omega\,\varepsilon_0} - j\varepsilon_{r,i}\tan(\delta_i)$ with σ_i the layer conductivity and $\tan(\delta_i)$ its dielectric loss tangent. This also applies to metal layers with finite conductivity where the good conductor approximation from [11] may be followed (i.e. only the term due to conductivity must be considered). Considering complex permittivity, the integration of (1) will catch the ohmic and dielectric losses as well as radiated and surface wave power of all the modes. In this case the numerical integration is easier as the poles are complex (i.e. the SW are attenuating) and the singularity is not in the integration path anymore. The losses can therefore be obtained by subtracting the radiated power given in (7) to the integral of (1) on the whole domain.

To have an accurate expression of the total efficiency, the conductive losses of the antenna itself should be accounted for. Equation (1) assumes that the antenna is a lossless sheet of current. Considering an antenna of thickness th, the resistance per unit length of the antenna can be expressed as

$$R' = \frac{1}{\sigma\, 2(W+th)\delta} \tag{10}$$

with δ the skin depth of the metal. The losses due to the finite conductivity of the antenna are given by

$$P_{Ant} = \int_0^L R'(x)\, I_x^2(x)\, dz. \tag{11}$$

For the case of the current distribution given in (3):

$$P_{Ant} = \int_0^L R'\, J_0^2 \sin^2\left(\frac{\pi x}{L}\right) dz = \frac{J_0^2}{\sigma\cdot(W+th)\cdot\delta}\frac{L}{4}. \tag{12}$$

The antenna efficiency e_r can be expressed as

$$e_r = \frac{P_{rad}}{P_{rad}+P_{material}+P_{SW}} = \frac{P_{rad}}{P_{out}+P_{Ant}} \tag{13}$$

with P_{rad} the radiated power, given in (7), P_{SW} the power coupled to surface waves and $P_{material}$ the material losses (i.e. due to substrate conductivity, dielectric losses or metal finite conductivity). P_{out} is the total power that leaves out the antenna, as given in (1), while P_{Ant} accounts for the losses due to the antenna conductivity, as given in (12). It should be noted that the efficiency, as considered in this paper, do not account for the input mismatch.

III. Application to Unshielded Antennas

In this section, the analytical method for efficiency assessment is applied to an unshielded AoC (i.e. no metal plane is separating the BEOL from the metal-backed substrate). For this analysis a typical Si chip stack is considered as shown in Fig. 2.

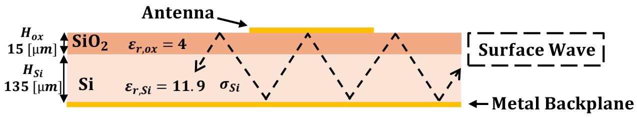

Fig. 2. Unshielded antenna stack considered.

For this material stack, considering a PEC backplane, the expressions of $D_{TM}(\beta)$ and $D_{TE}(\beta)$ given in (6) can be used with

$$\Gamma_{\mathrm{TE}} = \frac{\frac{k_{z,ox}-k_{z,Si}}{k_{z,ox}+k_{z,Si}} - e^{-2jk_{z,Si}H_{Si}}}{1+\frac{k_{z,ox}-k_{z,Si}}{k_{z,ox}+k_{z,Si}}\, e^{-2jk_{z,Si}H_{Si}}}\, e^{-2jk_{z,ox}H_{ox}} \tag{14.a}$$

$$\Gamma_{\mathrm{TM}} = \frac{-\frac{\varepsilon_{r,ox}k_{z,Si}-\varepsilon_{r,Si}k_{z,ox}}{\varepsilon_{r,ox}k_{z,Si}+\varepsilon_{r,Si}k_{z,ox}} + e^{-2jk_{z,Si}H_{Si}}}{1-\frac{\varepsilon_{r,ox}k_{z,Si}-\varepsilon_{r,Si}k_{z,ox}}{\varepsilon_{r,ox}k_{z,Si}+\varepsilon_{r,Si}k_{z,ox}}\, e^{-2jk_{z,Si}H_{Si}}}\, e^{-2jk_{z,ox}H_{ox}} \tag{14.b}$$

where the subscripts *ox* and *Si* refer to the SiO_2 and Si layers.

From (9), it can be shown that, for this stack, the residue extraction of the fundamental SW mode in a lossless scenario leads to (15) (not demonstrated here), where $\mathrm{s_{ox}} = \sin(H_{ox}k_{z,ox})$, $\mathrm{c_{ox}} = \cos(H_{ox}k_{z,ox})$, $\mathrm{s_{Si}} = \sin(H_{Si}k_{z,Si})$, $\mathrm{c_{Si}} = \cos(H_{Si}k_{z,Si})$. The explicit value of the derivative is not given here.

The propagation constant of the TM_0 SW mode β_{TM0} for the multi-layer stack considered here was extracted using [12]. For the stack analysed here, it can be shown using [12] that (15) accounts for all the SW power up to ~165 GHz, above what the TE_1 SW mode should be considered. The expression of the residue for the higher order modes is not derived in this paper but can be found the same way.

To account for the ohmic losses in the substrate, the integral of (1) should be numerically solved. If copper is considered as the backplane, the metal losses from this backplane can be shown to be negligible w.r.t. the substrate losses, even for a 5 kΩcm Si. A perfect electrical conductor (PEC) backplane is then considered to avoid complicating the expressions and allows to use (14) in the integral of (1).

Fig. 3 shows the result of the applied analytical method on the stack depicted in Fig. 2 for dipoles on three loss scenarios: lossless materials – lossy substrate – lossy substrate and antenna. This is done for three values of Si substrate resistivity: {5 kΩcm, 100 Ωcm, 20 Ωcm}. The extrema correspond to typical resistivity values used in Si-based processes: High-resistivity and standard Si, respectively [12]. The analytical method is validated with full-wave simulations in Fig. 3. Dipoles were simulated on the same stack using ADS from Keysight with a Method of Moment solver. It can be noted that the length of the dipoles for the full-wave simulation was computed such that $L = \lambda_0/(2\sqrt{\varepsilon_{r,eff}})$, with $\varepsilon_{r,eff}$ the effective permittivity. The expressions of the effective permittivity for a single grounded dielectric slab from [13] was used:

$$\varepsilon_{r,eff} = \frac{\varepsilon_r+1}{2} + \frac{\varepsilon_r-1}{2\sqrt{1+\frac{10H}{W}}} \tag{16}$$

with ε_r considered equal to 5 for an antenna at the SiO_2/air interface in the stack shown in Fig. 2. It can be shown that for this parameter a sine current function is obtained on the dipole.

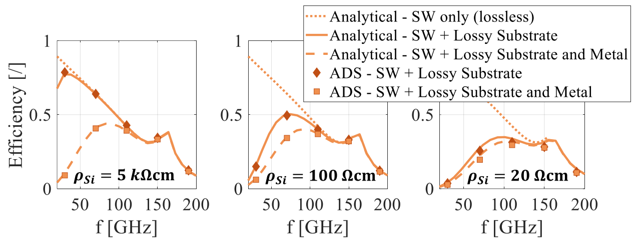

Fig. 3. Dipole efficiency with $W = 15$ µm, $th = 3$ µm for the unshielded stack of Fig. 2 with various substrate resistivity values.

The numerical integration was performed in Matlab and for the case of the lossy antenna, 3 µm-thick copper is considered as metal for the antenna ($\sigma_{Cu} = 5.8\cdot 10^7$ S/m). Good agreement between ADS and the analytical method is observed, validating the approach of the analytical expression. The relative impact of each loss mechanism can be observed depending on the substrate resistivity. For a 5 kΩcm substrate, the antenna losses dominate on the substrate and SW losses up to 110 GHz where the SW losses take the lead. For the 20 Ωcm Si the substrate losses dominate, and the antenna losses have almost no impact. Above 130 GHz, the SW losses dominate. The 100 Ωcm Si substrate shows an in-between behaviour as expected.

IV. Application to BEOL Shielded Antennas

In this section, the analytical method for efficiency assessment is applied to a shielded AoC (i.e. a metal plane is separating the BEOL from the substrate). For this analysis a typical Si chip stack is considered as shown in Fig. 4.

$$P_{TM0} = \mathbb{R}\left\{\frac{\beta_{TM0}}{8\pi}\int_0^{2\pi}\cos^2(\phi)\left|\tilde{J}_x(\beta_{TM0},\phi)\right|^2 d\phi\, \frac{(\varepsilon_{r,ox}\, k_{z,Si}\, \mathrm{c_{ox}}\, \mathrm{s_{Si}} + \varepsilon_{r,Si}\, k_{z,ox}\, \mathrm{c_{Si}}\, \mathrm{s_{ox}})\, k_{z,0}\, k_{z,ox}}{\frac{\partial}{\partial\beta}(j\varepsilon_{r,ox}\, k_{z,ox}k_{z,Si}\, \mathrm{c_{ox}}\, \mathrm{s_{Si}} + j\, \varepsilon_{r,Si}\, k_{z,ox}^2 \mathrm{c_{Si}}\, \mathrm{s_{ox}} - \varepsilon_{r,ox}^2\, k_{z,0}k_{z,Si}\mathrm{s_{Si}}\, \mathrm{s_{ox}} + \varepsilon_{r,ox}\, \varepsilon_{r,Si}\, k_{z,0}k_{z,ox}\mathrm{c_{Si}}\, \mathrm{c_{ox}})\big|_{\beta_{TM0}}}\right\} \tag{15}$$

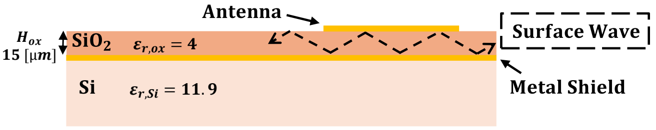

Fig. 4. Shielded antenna stack considered.

For a typical shielded AoC design, the bottom copper (σ_{Cu} =5.8 · 10^7S/m) layers of the BEOL are stacked to form a metal shield of 1 to 2 µm-thick depending on the process [14]. At 50 GHz, the skin depth of copper is equal to ~300 nm, which is much thinner than the shield thickness. It can therefore be approximated above this frequency that the fields generated by the antenna are confined in the SiO_2/air region and do not interact with the Si underneath the shield. The situation can then be simplified to a grounded dielectric slab with lossy metal. The expressions of $D_{TM}(\beta)$ and $D_{TE}(\beta)$ given in (6) can be used to compute the Green's function with:

$$\Gamma_{\mathrm{TE}} = \frac{k_{z,ox}-k_{z,m}}{k_{z,ox}+k_{z,m}}\, e^{-2jk_{z,ox}H_{ox}} \tag{17.a}$$

$$\Gamma_{\mathrm{TM}} = -\frac{\varepsilon_{r,ox}\, k_{z,m}-\varepsilon_{r,m}\, k_{z,ox}}{\varepsilon_{r,ox}\, k_{z,m}+\varepsilon_{r,m}\, k_{z,ox}}\, e^{-2jk_{z,ox}H_{ox}} \tag{17.b}$$

where the subscripts *ox* and *m* refer to the SiO_2 and metal layers. $\varepsilon_{r,m}$ is then the complex permittivity of the lossy shield whose expression can be obtained as explained in Section II.C.

After the simplifications given above, the power coupled to the fundamental SW mode reduces to the residue extraction of a grounded dielectric slab given in (18). An equivalent expression can be found in [8]. The TM_0 propagation constant β_{TM0} can be extracted using [12]. For the slab considered here, (18) accounts for all the SW power up to ~3 THz and is well sufficient for the frequency range targeted in this work.

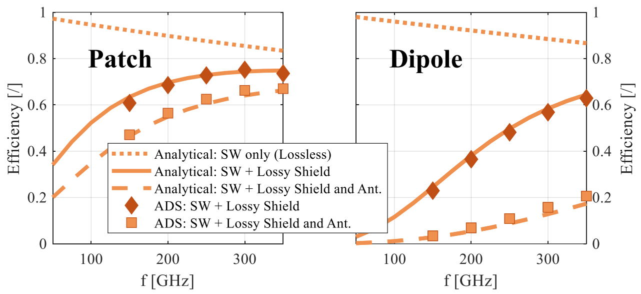

Fig. 5. Patch and dipole efficiency for the shielded stack of Fig. 4.

Fig. 5 shows the results of the applied analytical method on the stack depicted in Fig. 3 for both a patch and a dipole on three loss scenarios: lossless materials – lossy shield – lossy shield and antenna. In this figure, patches and dipoles have been simulated on a grounded dielectric slab with a copper shield in ADS. The length of the dipoles for the full-wave simulation was computed such that $L = \lambda_0/(2\sqrt{\varepsilon_{r,eff}})$ and using (16) to compute $\varepsilon_{r,eff}$ with the relative permittivity of the SiO_2, $\varepsilon_r = \varepsilon_{r,ox}$. For the patch, the dimensions given in [16] have been used.

The numerical integration was performed in Matlab and for the case of the lossy antenna, 3 µm-thick copper is considered for the antenna (σ_{Cu} =5.8· 10^7S/m). Again, good agreement between ADS and the analytical method is observed up to 350 GHz. The relative impact of each loss mechanism can be observed for both antennas. In the case of shielded AoCs, the power coupled to SW is way lower than for the unshielded case as expected since the backplane is closer to the source. The main contributors to the total losses are the copper backplane and antenna losses that cause a drop in efficiency, especially at low frequency. It can also be noted that the losses in the antenna itself are higher for the dipole since it is made of a thinner metal strip (i.e. W for the dipole is fixed to 5 µm in Fig. 5 while for the patch it is worth several tens of microns and is varying with frequency as given in [16]).

V. Conclusion

In this article, a systematic analysis tool for computing the efficiency of AoC with a prior knowledge on the material stack and current distribution is proposed. Expressions for AoC efficiency are derived for two widely used antenna types — patch and dipole antennas with rectangular current distributions following a sine pattern— but the methodology described is generalizable to any planar current distribution and lossy material stack. The model is validated with full-wave simulation in ADS from Keysight for both a shielded and unshielded silicon chip stack with typical dimensions (i.e. with and without a metal plane shielding the antenna from the substrate). In both cases, the model allows with reliability to quantify the impact of each loss source in the AoC design. It may enable AoC designers to evaluate antenna efficiency and effectively compare design options without relying extensively on numerous full-wave simulations in a predesign phase.

References

[1] B. Sievert et al., 54th EuMC, Paris, France, pp. 696-699, 2024.
[2] F. Gianesello et al., Antenna-in-Package Technology and Applications, IEEE, pp. 179-218, 2020.
[3] Y. P. Zhang et al., IEEE Trans. Antenn. Propag., vol. 57, no. 10, pp. 2830-2841, Oct. 2009.
[4] M. K. Hedayati et al., IEEE Access, vol. 7, pp. 43190-43204, 2019.
[5] R. Karim et al., IEEE Access, vol. 8, pp. 219577-219610, 2020.
[6] D. R. Jackson et al., IEEE Trans. Antenn. Propag., vol. 39, no. 3, pp. 407-410, March 1991.
[7] D. M. Pozar, Electronic Letters, Vol. 26, No. 13, 954-956, June 1990.
[8] P. Perlmutter et al., IEEE Trans. Antenn. Propag., vol. 33, no. 3, pp. 301-311, March 1985.
[9] Mosig, J. R., Numerical Techniques for Microwave and Millimeter-Wave Passive Structures, T. Itoh, pp. 133-213, 1989.
[10] J. Cavillot, PhD thesis, Louvain-la-Neuve, Belgium, 2021.
[11] R. F. Harrington, Time-Harmonic Electromagnetic Fields, New York: McGraw-Hill, pp. 51-53, 1981.
[12] L. Delait et al., IEEE APMC, Bali, Indonesia, pp. 635-637, 2024.
[13] M. V. Schneider, Bell System Technology Journal, Vol.48, pp. 1421-1444, May–June 1969.
[14] Y. Yang et al., IEEE Trans. Microw. Theory Tech., vol. 64, no. 12, pp. 4241-4249, Dec. 2016.
[15] D. M. Pozar, Microwave Engineering. 4th Edition, John Wiley & Sons, Inc., Hoboken, pp.135-140, 2012.
[16] C. A. Balanis, Antenna Theory Analysis and Design, 2nd Edition, John Wiley & Sons, Inc., New York, pp. 816-842, 1997.

$$P_{TM0} = \mathbb{R}\left\{ \frac{1}{8\pi}\frac{\eta_0}{k_0}\int_0^{2\pi}\cos^2(\phi)\,\left|\tilde{J}_x(\beta_{TM0},\phi)\right|^2 d\phi \cdot \frac{k_{z,ox}\,k_{z,0}}{-\frac{j}{k_{z,ox}} - j\,H_{ox}\cot(H_{ox}k_{z,ox}) + H_{ox}\,\varepsilon_{r,ox}\frac{k_{z,0}}{k_{z,ox}} - \frac{\varepsilon_{r,ox}}{k_{z,0}}\cot(H_{ox}k_{z,ox})}\right\} \tag{18}$$